Hindawi Publishing Corporation
Shock and Vibration
Volume 2015, Article ID 365084, 10 pages
http://dx.doi.org/10.1155/2015/365084

Research Article

Numerical Analysis and Demonstration: Transmission Shaft Influence on Meshing Vibration in Driving and Driven Gears

Xu Jinli, Su Xingyi, and Peng Bo

Wuhan University of Technology, Wuhan 430070, China

Correspondence should be addressed to Su Xingyi; sxy19900314@126.com

Received 23 November 2014; Accepted 3 April 2015

Academic Editor: Wen Long Li

The variable axial transmission system composed of universal joint transmission shafts and a gear pair has been applied in many engineering fields. In the design of a drive system, the dynamics of the gear pair have been studied in detail. However few have paid attention to the effect on the system modal characteristics of the gear pair, arising from the universal joint transmission shafts. This work establishes a torsional vibration mathematical model of the transmission shaft, driving gear, and driven gear based on lumped masses and the main reducer system assembly of a CDV (car-based delivery vehicle) car. The model is solved by the state space method. The influence of the angle between transmission shafts and intermediate support stiffness on the vibration and noise of the main reducer is obtained and verified experimentally. A reference for the main reducer and transmission shaft design and the allied parameter matching are provided.

1. Introduction

In the 1970s, to meet customer demand, the crossover was modified from cars in Europe and the United States. It stemmed from SUVs, gradually developed into an arbitrary combination of car, SUV, MPV, and pick-up. It set the comfort, fashion, and appearance standards for such cars; it had the control of an SUV and the capacity of an MPV internally. Crossovers are divided into SAV, CDV, vans, and other models. In recent years the production and sales of crossovers have developed rapidly in China. The technology has also been greatly improved through absorption and digestion. However the coupling technology between the transmission shafts on the chassis and gears in the main reducer has been a hot research topic for the industry. There remains the effect on car NVH due to their coupling. Qualitative research into the influence of transmission shaft angle and intermediate support stiffness on meshing vibration of gears remains sparse.

A CDV car produced in China suffers from excessive internal noise (60 db). The performance of an NVH does not meet the level required of a passenger vehicle. The main reason for this is shock and vibration from its transmission system [1, 2]. The transmission system of that car can be described as a "universal joint—transmission shaft—gear meshing system" (known as a variable axial transmission system). This kind of flexible transmission system can meet the requirements of torque output floating [3, 4]. There is no accurate quantitative analysis on angle between the transmission shafts according to the CDV car. In the situation of freedom (car suspension), the initial installation angle changes from 0° to 10°. Without considering influence of car weight and load on the initial installation angle, angle between the transmission shafts changes during driving, while few studies have been involved in quantitative analysis on intermediate support stiffness. The stiffness value (600 N/mm~700 N/mm) is determined by analogy and experience analysis, especially the mutual coupling effect of installation angle between transmission shafts and intermediate support stiffness on vibration of driving and driven gear is less involved currently.

This work focuses on the drive shaft—rear axle main reducer and gear [5, 6] system of the vehicle, creates a torsional vibration model, and solves its equations by the lumped mass method. Influences of transmission shaft angle and intermediate support stiffness on the meshing vibration of both driving and driven gears are studied [7, 8], and the installation angle and intermediate support stiffness are

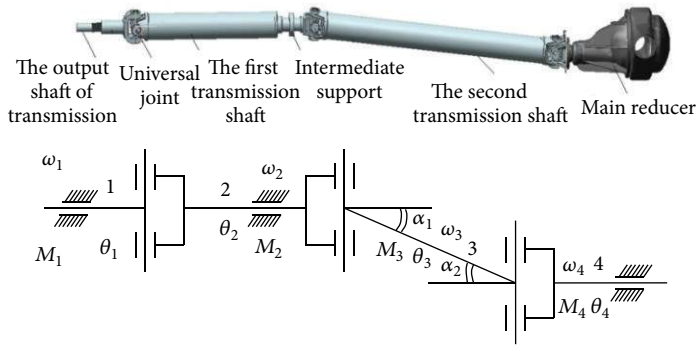

Figure 1: Universal transmission device structure investigated.

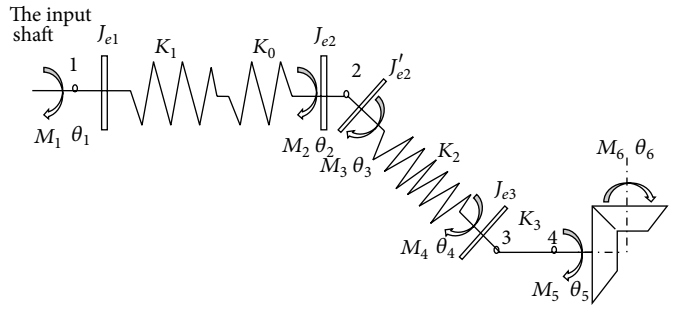

Figure 2: Torsional vibration analysis model of the transmission shaft, driving gear, and driven gear system.

quantified. Vibration and shock from the variable axial transmission system are reduced, thereby improving the vehicle's performance. This study provides useful reference for the design of automobile chassis.

2. The "Transmission Shaft—Driving Gear and Driven Gear" Mathematical Model

The key factors affecting vibration and noise in the main reducer are the driving gear and driven gear's meshing movement [9, 10]. It is also one of the factors influencing vehicle NVH. As an elastic mechanical system, both the driving gear and driven gear will have vibration responses to dynamic excitation during transmission time. The dynamic excitation of the driving and driven gears mainly includes transmission shaft input excitation and road load excitation [11]. As a result, when researching the problem of vibration and noise caused by the meshing of the driving gear and driven gear, it is important to determine the main characteristics of both of their excitations.

2.1. Establishing a Torsional Vibration Model: "Transmission Shaft—Driving Gear and Driven Gear". The "transmission shaft—driving gear and driven gear" system is analyzed dynamically. The complex mechanical system is simplified by the lumped mass method. The torsional vibration mathematical analysis model for this elastic mechanical system is established by Lagrange's equation: because the system components are both numerous and complex in structure, the form of movement is not only translational but also rotational. It is necessary to calculate only after simplification. In the torsional vibration model, all components connected with the rotating shaft are treated as absolutely rigid bodies with a moment of inertia. The shaft section moment of inertia equivalent is transferred to the two ends of the shaft. The rigid bodies, after equivalent treatment, are connected by a series of equivalent bodies with elasticity and no moment of inertia; thus an equivalent analysis model of the vehicle's variable axial transmission system is established. The structure of the vehicle transmission shaft and the main reducer investigated here is shown in Figure 1.

The torsional vibration mathematical model of the transmission shaft, driving gear, and driven gear system is established by considering the transmission system torsional vibrations: a simplified model is shown in Figure 2.

The transmission shaft comprises three cross-shaft universal joints. Suppose that there is a model with a node in each universal joint (nodes 1, 2, and 3). Torque transferred from the engine by the gearbox acts on node 1. The two section transmission shafts are simplified as torsional springs and mass points. The intermediate support is simplified as a torsional spring of stiffness K_0. The output end of the second transmission shaft is connected to the driving gear; because the driving gear shaft stiffness is large, the influence of the driving gear shaft on torsional vibration of the system is ignored. Load torque is simplified and applied to the main reducer's driven gear. According to Lagrange's equation and Newton's second law, the corner is selected as the origin: the generalised coordinates are expressed as

$q = (\theta_1, \theta_2, \theta_3, \theta_4, \theta_5, \theta_6)$. The system's torsional vibration model is

$$\begin{aligned} J_{e1}\ddot{\theta}_1 - K_1(\theta_2 - \theta_1) - C_1\left(\dot{\theta}_2 - \dot{\theta}_1\right) &= M_1, \\ J_{e2}\ddot{\theta}_2 + K_1(\theta_2 - \theta_1) + C_1\left(\dot{\theta}_2 - \dot{\theta}_1\right) &= -M_2, \\ J'_{e2}\ddot{\theta}_3 - K_2(\theta_4 - \theta_3) - C_2\left(\dot{\theta}_4 - \dot{\theta}_3\right) &= M_3, \\ J_{e3}\ddot{\theta}_4 + K_2(\theta_4 - \theta_3) + C_2\left(\dot{\theta}_4 - \dot{\theta}_3\right) &= -M_4, \\ J_{\text{driving}}\ddot{\theta}_5 + T_n &= M_5, \\ J_{\text{driven}}\ddot{\theta}_6 - T_n &= -M_6, \end{aligned} \tag{1}$$

where J_{e1} is the equivalent polar moment of inertia of the first transmission shaft at node 1 of the universal joint; K_1 is the series equivalent stiffness of the first transmission shaft tube and its intermediate support; C_1 is the damping coefficient of the first transmission shaft; J_{e2} is the equivalent polar moment of inertia of the first transmission shaft at node 2 of the universal joint; is the equivalent polar moment of inertia of the second transmission shaft at node 2 of the universal joint; K_2 is the series equivalent stiffness of the second transmission shaft tube and its intermediate support; C_2 is the damping coefficient of the second transmission shaft; J_{e3} is the equivalent polar moment of inertia of the second transmission shaft at node 3 of the universal joint; J_{driving} is the equivalent polar moment of inertia of the main reducer driving gear; J_{driven} is the equivalent polar moment of inertia of the main reducer driven gear; T_n is the dynamic meshing force of the driving gear and driven gear; M_1, M_6 are the engine output torque and the equivalent torque loading on the driven gear.

Equation (1) is transferred to the torsional vibration equation of the system in matrix form:

$$\{J_e\} \cdot \{\ddot{q}\} + \{C_e\}\{\dot{q}\} + \{K_e\}\{q\} = \{M(t)\}, \tag{2}$$

where $\{J_e\}$ is the equivalent polar inertia matrix of the system; $\{C_e\}$ is the equivalent damping matrix; $\{K_e\}$ is the equivalent stiffness matrix; and $\{M(t)\}$ is the torque vector matrix of the system. The dynamic meshing force between the driving gear and the driven gear is as follows [12, 13]:

$$T_n = K_m \cdot (\theta_5 - \theta_6) + C_m \cdot \left(\dot{\theta}_5 - \dot{\theta}_6\right), \tag{3}$$

where K_m, C_m are the average meshing stiffness of reverse and average meshing damping between gears.

When the power transmission shaft is stable, the rotation angle between transmission shaft axes [14] (Figures 1 and 2) is

$$\begin{aligned} \tan\theta_2 &= \tan\theta_3 \cdot \cos\alpha_1, \\ \tan\theta_4 &= \tan\theta_3 \cdot \cos\alpha_2, \\ \omega_3 &= \frac{\cos\alpha_1}{1 - \sin^2\alpha_1 \cdot \cos^2\theta_2}\omega_2, \\ \omega_4 &= \frac{\cos\alpha_2}{1 + \sin^2\theta_3 \cdot \left(\cos^2\alpha_2 - 1\right)}\omega_3. \end{aligned} \tag{4}$$

The relationship between the different transmission shaft torques is as follows:

$$M_i\omega_i = M_l\omega_l. \tag{5}$$

Uniting (1) to (5) allows the torsional vibration analysis model to be numerically solved.

2.2. Numerical Solution of the System Torsional Vibration Model. To obtain the numerical solution, (2) is solved by a combination of state space method and Runge-Kutta method. The state space method is analytical and is a comprehensive method for the dynamic characteristics of the system in modern control theory. The analysis process sets state space variables which can identify and characterise the system. Then the dynamic characteristics of the system are identified by the first-order differential equations composed of the state space variables. The transfer function between system input and output can be obtained by the state space equation. If the input is known, then the value of the state variables can determine the changing characteristics of the output completely.

Set the output variable of system:

$$\begin{aligned} Y_1 &= Z_2, \\ Y_2 &= Z_4, \\ Y_3 &= Z_6, \\ Y_4 &= Z_8, \\ Y_5 &= Z_{10}, \\ Y_6 &= Z_{12}. \end{aligned} \tag{6}$$

Select the state space variables:

$$\begin{aligned} Z_1 &= \theta_1, \\ Z_2 &= \dot{\theta}_1, \\ Z_3 &= \theta_2, \\ Z_4 &= \dot{\theta}_2, \\ Z_5 &= \theta_3, \\ Z_6 &= \dot{\theta}_3, \\ Z_7 &= \theta_4, \\ Z_8 &= \dot{\theta}_4, \\ Z_9 &= \theta_5, \\ Z_{10} &= \dot{\theta}_5, \\ Z_{11} &= \theta_6, \\ Z_{12} &= \dot{\theta}_6. \end{aligned} \tag{7}$$

Equation (2) is transformed into the state space expression [15]:

$$
\begin{bmatrix} \dot{\theta}_1 \\ \ddot{\theta}_1 \\ \dot{\theta}_2 \\ \ddot{\theta}_2 \\ \dot{\theta}_3 \\ \ddot{\theta}_3 \\ \dot{\theta}_4 \\ \ddot{\theta}_4 \\ \dot{\theta}_5 \\ \ddot{\theta}_5 \\ \dot{\theta}_6 \\ \ddot{\theta}_6 \end{bmatrix} = \begin{bmatrix} \dot{Z}_1 \\ \dot{Z}_2 \\ \dot{Z}_3 \\ \dot{Z}_4 \\ \dot{Z}_5 \\ \dot{Z}_6 \\ \dot{Z}_7 \\ \dot{Z}_8 \\ \dot{Z}_9 \\ \dot{Z}_{10} \\ \dot{Z}_{11} \\ \dot{Z}_{12} \end{bmatrix}
$$

$$
= \begin{bmatrix}
0 & 1 & 0 & 0 & 0 & 0 & 0 & 0 & 0 & 0 & 0 & 0 \\
\frac{-k_1}{J_{e1}} & \frac{-c_1}{J_{e1}} & \frac{k_1}{J_{e1}} & \frac{c_1}{J_{e1}} & 0 & 0 & 0 & 0 & 0 & 0 & 0 & 0 \\
0 & 0 & 0 & 1 & 0 & 0 & 0 & 0 & 0 & 0 & 0 & 0 \\
\frac{k_1}{J_{e2}} & \frac{c_1}{J_{e2}} & \frac{-k_1}{J_{e2}} & \frac{-c_1}{J_{e2}} & 0 & 0 & 0 & 0 & 0 & 0 & 0 & 0 \\
0 & 0 & 0 & 0 & 0 & 1 & 0 & 0 & 0 & 0 & 0 & 0 \\
0 & 0 & 0 & 0 & \frac{-k_2}{J'_{e2}} & \frac{-c_2}{J'_{e2}} & \frac{k_2}{J'_{e2}} & \frac{c_2}{J'_{e2}} & 0 & 0 & 0 & 0 \\
0 & 0 & 0 & 0 & 0 & 0 & 0 & 1 & 0 & 0 & 0 & 0 \\
0 & 0 & 0 & 0 & \frac{k_2}{J_{e3}} & \frac{c_2}{J_{e3}} & \frac{-k_2}{J_{e3}} & \frac{-c_2}{J_{e3}} & 0 & 0 & 0 & 0 \\
0 & 0 & 0 & 0 & 0 & 0 & 0 & 0 & 0 & 1 & 0 & 0 \\
0 & 0 & 0 & 0 & 0 & 0 & 0 & 0 & \frac{-k_m}{J_{\text{driving}}} & \frac{-c_m}{J_{\text{driving}}} & \frac{k_m}{J_{\text{driving}}} & \frac{c_m}{J_{\text{driving}}} \\
0 & 0 & 0 & 0 & 0 & 0 & 0 & 0 & 0 & 0 & 0 & 1 \\
0 & 0 & 0 & 0 & 0 & 0 & 0 & 0 & \frac{k_m}{J_{\text{driven}}} & \frac{c_m}{J_{\text{driven}}} & \frac{-k_m}{J_{\text{driven}}} & \frac{-c_m}{J_{\text{driven}}}
\end{bmatrix} \cdot \begin{bmatrix} Z_1 \\ Z_2 \\ Z_3 \\ Z_4 \\ Z_5 \\ Z_6 \\ Z_7 \\ Z_8 \\ Z_9 \\ Z_{10} \\ Z_{11} \\ Z_{12} \end{bmatrix}
$$

$$
+ \begin{bmatrix}
0 & 0 & 0 & 0 & 0 & 0 \\
\frac{1}{J_{e1}} & 0 & 0 & 0 & 0 & 0 \\
0 & 0 & 0 & 0 & 0 & 0 \\
0 & -\frac{1}{J_{e2}} & 0 & 0 & 0 & 0 \\
0 & 0 & 0 & 0 & 0 & 0 \\
0 & 0 & \frac{1}{J'_{e2}} & 0 & 0 & 0 \\
0 & 0 & 0 & 0 & 0 & 0 \\
0 & 0 & 0 & -\frac{1}{J_{e3}} & 0 & 0 \\
0 & 0 & 0 & 0 & 0 & 0 \\
0 & 0 & 0 & 0 & \frac{1}{J_{\text{driving}}} & 0 \\
0 & 0 & 0 & 0 & 0 & 0 \\
0 & 0 & 0 & 0 & 0 & -\frac{1}{J_{\text{driven}}}
\end{bmatrix} \cdot \begin{bmatrix} M_1 \\ M_2 \\ M_3 \\ M_4 \\ M_5 \\ M_6 \end{bmatrix}. \tag{8}
$$

At the same time, the state space expression for the torsional mathematical analysis model output variable is obtained:

$$\begin{bmatrix} Y_1 \\ Y_2 \\ Y_3 \\ Y_4 \\ Y_5 \\ Y_6 \end{bmatrix} = \begin{bmatrix} Z_2 \\ Z_4 \\ Z_6 \\ Z_8 \\ Z_{10} \\ Z_{12} \end{bmatrix} = \begin{bmatrix} 0 & 1 & 0 & 0 & 0 & 0 & 0 & 0 & 0 & 0 & 0 & 0 \\ 0 & 0 & 0 & 1 & 0 & 0 & 0 & 0 & 0 & 0 & 0 & 0 \\ 0 & 0 & 0 & 0 & 0 & 1 & 0 & 0 & 0 & 0 & 0 & 0 \\ 0 & 0 & 0 & 0 & 0 & 0 & 0 & 1 & 0 & 0 & 0 & 0 \\ 0 & 0 & 0 & 0 & 0 & 0 & 0 & 0 & 0 & 1 & 0 & 0 \\ 0 & 0 & 0 & 0 & 0 & 0 & 0 & 0 & 0 & 0 & 0 & 1 \end{bmatrix} \cdot \begin{bmatrix} Z_1 \\ Z_2 \\ Z_3 \\ Z_4 \\ Z_5 \\ Z_6 \\ Z_7 \\ Z_8 \\ Z_9 \\ Z_{10} \\ Z_{11} \\ Z_{12} \end{bmatrix}. \tag{9}$$

The parameters of the mathematical model are substituted into the state space expression. The torsional vibration response of the system can then be obtained by Runge-Kutta method.

3. Determining Parameters in the Model

3.1. Determining Coefficients in the Model. The transmission shaft's main parameters for the car researched here are listed in Table 1. The main parameters of both driving and driven gears are listed in Table 2.

The torsional stiffness of the transmission shaft is

$$K_i' = \frac{GI_P}{L}\ \mathrm{N \cdot m/rad}. \tag{10}$$

G is the shear modulus, $7.94 \times 10^{10}\ \mathrm{N{\cdot}m^{-2}}$; and L is the length of the shaft.

The transmission shaft of the car is modelled as a thin-walled circular cross-section:

$$I_p \approx 2\pi d^3 (D - d) = 4.86 \times 10^{-6}\ \mathrm{m}^4. \tag{11}$$

The intermediate support and transmission shaft total equivalent torsional stiffness values are as follows [16]:

$$\frac{1}{K_i} = \frac{1}{K_O} + \frac{1}{K_i'}. \tag{12}$$

There are many calculation methods available for the linear meshing stiffness of gears: as far as accuracy is concerned, a single gear tooth's linear meshing stiffness is calculated by the ISO method. Results that have little difference to the actual meshing stiffness may be obtained by this method. The hypoid gears of Gleason are adopted in the main reducer of the vehicle with a gear meshing stiffness with a linear value [17]

$$k_{mb} = 1.84 \times 10^6\ \mathrm{N/m}. \tag{13}$$

The value of the gear's equivalent meshing damping is

$$C_m = 2\xi \sqrt{k_{mb} \left(\frac{1}{m_1} + \frac{1}{m_2} \right)}\ \mathrm{N \cdot s/m}. \tag{14}$$

m_1, m_2 are the driven and driving gear's qualities and ξ is the damping ratio, with a value of 0.1 here.

The average torsional stiffness of the gear is as follows:

$$K_m = \frac{K_{mb} \left(r_{b1}^2 + r_{b2}^2 \right)}{2 r_{b1}^2 r_{b2}^2} = 2.34 \times 10^3\ \mathrm{N \cdot m/rad}, \tag{15}$$

where r_{b1} is the pitch circle radius of the driven gear and r_{b2} is the pitch circle radius of the driving gear.

The equivalent polar moment of inertia of the first transmission shaft at node 1 of the universal joint is

$$J_{e1} = 0.5 \cdot \left(J_{sze1} + J_{cde1} \right) + J_{zce1}. \tag{16}$$

J_{sze1} is the first universal joint cross-shaft's equivalent polar moment of inertia about the first transmission axis; J_{cde1} is the first transmission shaft's equivalent polar moment of inertia about its geometric centre; J_{zce1} is the first joint shaft fork's equivalent polar moment of inertia about the first transmission axis.

The 3d model of transmission shaft and main reducer is imported into UG software. Values of J_{sze1}, J_{cde1}, and J_{zce1} are calculated by UG: the values are listed in Table 3.

According to (16) $J_{e1} = 0.309234412\ \mathrm{kg{\cdot}m^2}$. As the same, $J_{e2} = J_{e1} = 0.309234412\ \mathrm{kg{\cdot}m^2}$.

Using the same method, the cross-shaft and shaft fork's moments of inertia can be calculated: these act from the second universal joint and their values are listed in Table 4.

$J_{e2}' = 1.8665142935\ \mathrm{kg{\cdot}m^2}$, $J_{e3}' = 2.324507441\ \mathrm{kg{\cdot}m^2}$, $J_{\mathrm{driving}} = 1.236925720\ \mathrm{kg{\cdot}m^2}$, and $J_{\mathrm{driven}} = 0.027998012\ \mathrm{kg{\cdot}m^2}$.

The parameters for (1) can be found in Table 5.

3.2. Determination of Car Main Reducer External Excitation. Here, considering fluctuations in main reducer input torque and load torque, the input torque and load torque are set as follows [18]:

$$\begin{aligned} M_1(t) &= M_1 + \sigma \cos \omega_k t, \\ M_6(t) &= M_6 + \sigma \cos \omega_k t, \end{aligned} \tag{17}$$

where M_1 is the input torque from the engine; M_6 is the load torque; σ is the coefficient of torque fluctuation (its value is 0.1); and ω_k is the angular velocity of the transmission axis.

Table 1: Main parameters of the transmission shaft.

Parameters	Shear modulus G (GPa)	Length of the shaft L (mm)	Shaft tube section outside diameter D (mm)	Shaft tube section inside diameter d (mm)
First shaft	79.4	524	63.5	59.9
Second shaft	79.4	875	63.5	59.9

Table 2: Main parameters of gears.

Name and code	Driven gear		Driving gear
The number of teeth (Z)	41		8
Surface cone angle (DELTA-A)	$76^\circ\ 55'\ 40'' \approx 76.93^\circ$		$18^\circ\ 14'\ 10'' \approx 18.24^\circ$
Reference cone angle (DELTA-B)	$75^\circ\ 55'\ 50'' \approx 75.93^\circ$		$12^\circ\ 56' \approx 12.93^\circ$
Root angle (DELTA-F)	$70^\circ\ 16'\ 47'' \approx 70.28^\circ$		$12^\circ\ 2'\ 35'' \approx 12.04^\circ$
Offset distance		30 mm (lower)	
The average pressure angle (ALPHA)		$21^\circ\ 15' \approx 21.25^\circ$	
Pitch circle diameter (D)	170.601 mm		
Equivalent radius (R)	73.18 mm		20.5 mm
Mean spiral angle (BETA)	$26^\circ\ 46'\ 25'' \approx 26.77^\circ$		$49^\circ\ 59'\ 48'' \approx 49.9967^\circ$
Cutter diameter (BETA-R)		152.4 mm	
The gear width (BF)	25 mm		33.3 mm
Base circle diameter (Db)		Db = D * COS(ALPHA)	

Table 3: Values of J_{sze1}, J_{cde1}, and J_{zce1}.

Moment of inertia	J_{sze1}	J_{cde1}	J_{zce1}
About the x-axis	0.000538185	0.617267494	0.002713877
About the y-axis	0.000129689	0.001702246	0.000535828
About the z-axis	0.0005382	0.617267479	0.002981971

Table 4: Values of J'_{sze2}, J'_{cde2}, and J'_{zce2}.

Moment of inertia	J'_{sze2}	J'_{cde2}	J'_{zce2}
About the x-axis	0.342704517	3.720747326	0.342704517
About the y-axis	0.000541772	0.012791622	0.000541772
About the z-axis	0.342442366	3.731261792	0.342442366

Considering when the CDV car is running at an engine speed of 3500 rpm, $M_1 = 151.20$ N·m, the vibration and noise were large. The normal mass of the car is 1500 kg, and the wheel effective radius is 290 mm, giving $M_6 = 750$ N·m; the speed of transmission shaft is 2500 rpm.

4. Response Analysis of the System's Torsional Vibration

4.1. Effects of the Angle between the Axes on Vibration in the Main Reducer. Having established the mathematical relationship between the angle of the transmission shafts and the output variables of the state space using a MATLAB simulation, the system response curves for angular velocity and angular displacement are realised as shown in Figures 3 and 4.

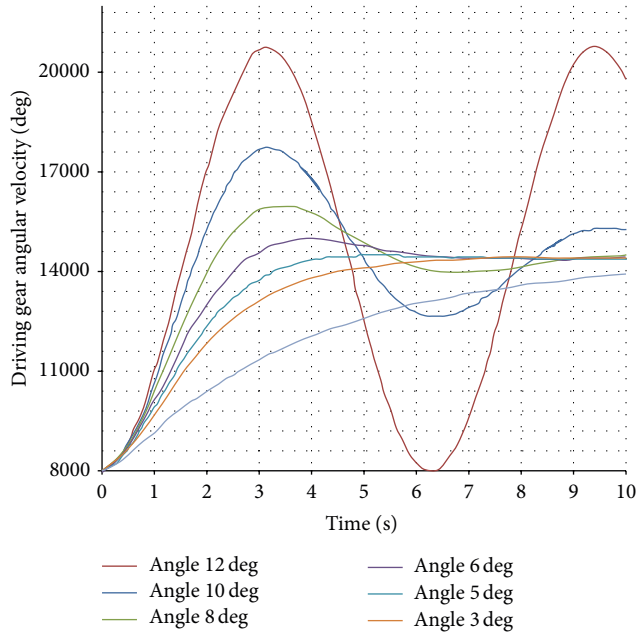

Figure 3: Response curve: driving gear angular velocity.

In Figure 3, the installation angle α is taking values of 0°, 3°, 5°, 6°, 8°, 10°, and 12° in turn. The transmission system consists of multiparts. During engine start-up phase, coupling effect between multiparts causes the change of angular velocity fluctuations at different installation angles, while angular velocity fluctuations are stable in a certain area and periodic vibrating by a certain time. When installation angle is 12°, the unstable time of fluctuation is longest and

Table 5: Main parameters of transmission system.

Name	Code	Parameters	Name	Code	Parameters
The series equivalent stiffness of the first transmission shaft's tube and its intermediate support	K_1	$\frac{7.36 \times 10^5 \times K_O}{7.36 \times 10^5 + K_O}$ N·m/rad	The series equivalent stiffness of the second transmission shaft's tube and its intermediate support	K_2	$\frac{4.41 \times 10^5 \times K_O}{4.41 \times 10^5 + K_O}$ N·m/rad
The damping coefficient of the first transmission shaft	C_1	0.002	The damping coefficient of the second transmission shaft	C_2	0.002
The equivalent polar moment of inertia of the first transmission shaft at node 1 of the universal joint	J_{e1}	0.309234412 kg·m^2	The equivalent polar moment of inertia of the first transmission shaft at node 2 of the universal joint	J_{e2}	0.309234412 kg·m^2
The equivalent polar moment of inertia of the second transmission shaft at node 2 of the universal joint	J'_{e2}	1.866514293 kg·m^2	The equivalent polar moment of inertia of the second transmission shaft at node 3 of the universal joint	J_{e3}	2.324507441 kg·m^2
The driving gear and driven gear's average meshing stiffness in reverse	K_m	2.48×10^3 N·m/rad	The driving gear and driven gear's average meshing damping	C_m	47.8 (N·s/m)
The equivalent polar moment of inertia of the main reducer driving gear	J_{driving}	1.236925720 kg·m^2	The equivalent polar moment of inertia of the main reducer driven gear	J_{driven}	0.027998012 kg·m^2

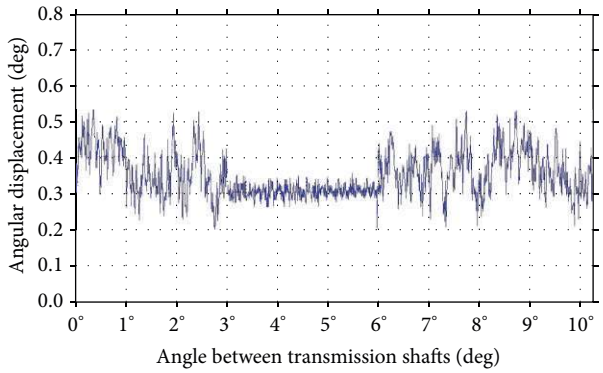

Figure 4: Response curve: driven gear angular displacement.

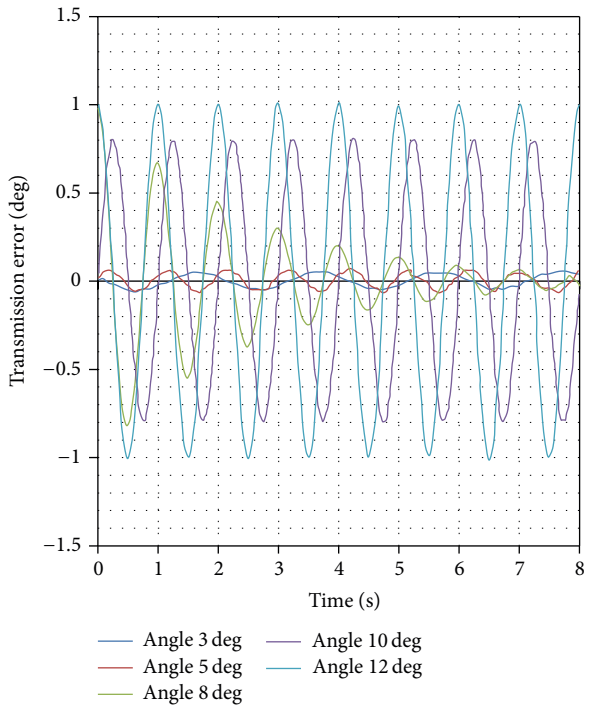

Figure 5: Transmission error: angular displacement—time curve.

stabilize fluctuation is largest. While angle is 5°~6°, driving gear can quickly enter smooth transmission and fluctuation of angular velocity is minimal.

The changes in the driven gear's angular displacement are shown in Figure 4. With an analysis of response curve and variation curve, it is seen that the angle between transmission shafts has an influence on vibration and noise in both gears. With the change in angle between the transmission shafts, the driven gear's amplitude of vibration increases at first from 0° to 3° and then decreases to a series of small fluctuations of stable amplitude at installation angles of 3° to 6°. When the angle increases, the torsional vibration intensifies.

From an analysis of Figure 5, when the transmission shaft stiffness is the same as that of its intermediate support, the transmission error fluctuates cyclically. Different angles between transmission shafts lead to different transmission accuracies. When the angle between the transmission shafts

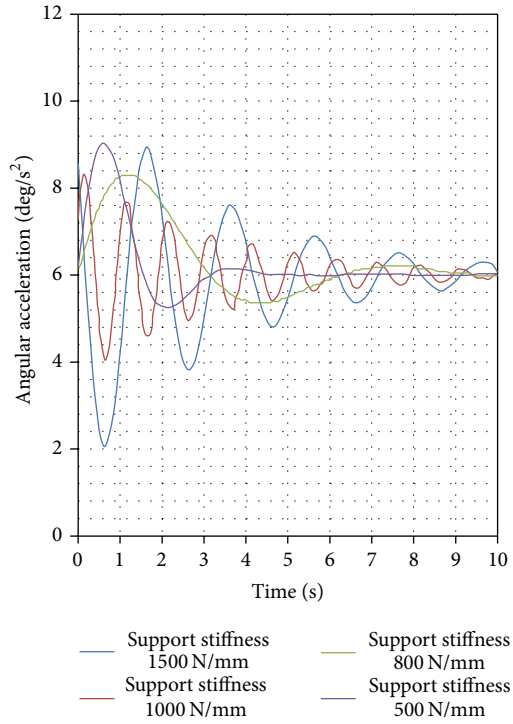

Figure 6: Angular acceleration plots for the driven gear for different stiffness values.

changes from 3° to 5°, the transmission error fluctuation is small. While the angle is 5°, the transmission error is minimised; therefore it affords a better transfer of engine speed through the universal joint. As a result, rear axle vibration and noise caused by speed fluctuation can be reduced. Based on the above analysis, the angle between transmission shafts not only influences the transmission characteristics of the shaft, but also influences angular speed fluctuation and torsional vibration of the gear system. To improve transmission system comfort, the design angle should be 5°.

4.2. The Response Analysis of Intermediate Support Stiffness on Main Reducer Vibration. In Figure 6, the input torque and load torque have cosine-momentum. With the intermediate support's stiffness changing, the angular acceleration of the driven gear will undergo cyclical fluctuations. In the simulation, the intermediate support is variable and is set to 500 N/mm, 800 N/mm, 1000 N/mm, and 1500 N/mm in turn, other settings remaining unchanged. Through comparative analysis of the four plots in Figure 6, the driven gear's angular acceleration fluctuations are different. When the intermediate support stiffness is 500 N/mm, the angular acceleration fluctuation is relatively stable. The effect on both gears' meshing vibration is smaller.

5. Experimental Verification

The main factor causing vibration is meshing of the gears. The vibration of the main reducer in the rear bridge directly affects NVH performance. Therefore, vibration of the main reducer and the NVH noise performance can reflect meshing vibration of the gears directly. To verify the validity of the study, intermediate support stiffness and installation angle between transmission shafts are changed in a full-scale car test. Through changes in the aforementioned factors, NVH performance status inside the car and vibration of the main reducer would verify the validity of the study in actual operating conditions.

The test systems comprised a portable vibration tester developed by Wuhan University of Technology for the automobile main reducer and a portable LMS.Test.Lab NVH noise tester from LMS Co., (Belgium).

The portable vibration testing system has four acquisition channels. One channel acquisition records the transmission shaft speed signal; the other two channels record vibration acceleration signals in the vertical and horizontal directions from the main reducer. The recorded signals are displayed as plots of speed and the main reducer vibration acceleration on the computer screen in real-time. The LMS.Test.Lab NVH noise tester can test noise inside the car in real-time and reflect the overall noise performance of the automobile.

The experiment does not change the box, car clutch, front and rear suspensions, or any other factors: the only changes were made to the installation angle between transmission shafts and the intermediate support stiffness. The automotive engine was run over its full working range of up to 6000 rpm. The experimental installation is shown in Figure 7 and vibration is tested by point-to-point measurement, which avoids the influence of other vibrations. The noise tester (LMS Co., Belgium) is used to verify the data of which the project always recorded two sets to allow later comparison.

When the angle between transmission shafts is 7°, the intermediate support stiffness is approximately 700 N/mm, and the experimental result is shown in Figure 8.

When the angle between transmission shafts is 5°, the intermediate support stiffness is approximately 500 N/mm, and the experimental result is shown in Figure 9.

To further verify the effects of a change in installation angle and intermediate support stiffness on the rear axle, the experiment also tests the NVH (noise) inside the vehicle. The results are shown in Figure 10.

Comparing Figures 8 and 9, when the installation angle is 5° and the intermediate support stiffness is 500 N/mm, the effect on the rear axle vibration is obviously smaller. Seen from Figure 10, when the transmission shaft angle and intermediate support stiffness are changed, the NVH performance inside the car improved. Through experimental verification, data simulation, and analysis the data coincide with experimental verification thereof.

6. Conclusion

The research shows that the angle between transmission shafts has a great influence on vibration and shock in the rear axle main reducer. The numerical matching of the relationships between angle, intermediate support stiffness, and gears can be found by numerical solution. The angle between transmission shafts and the intermediate support stiffness can then be quantified. According to the CDV car studied

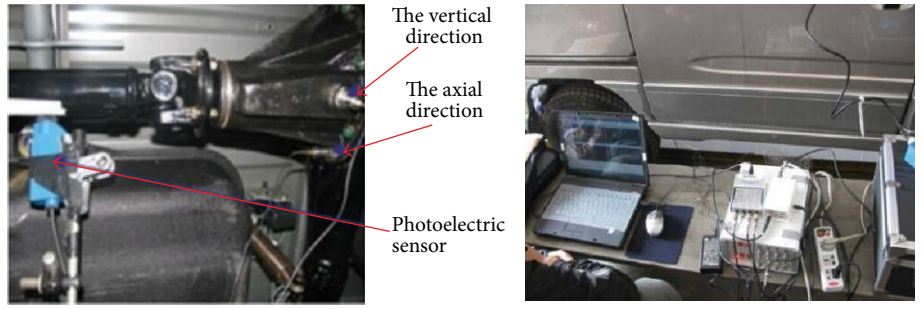

Figure 7: Experimental installation.

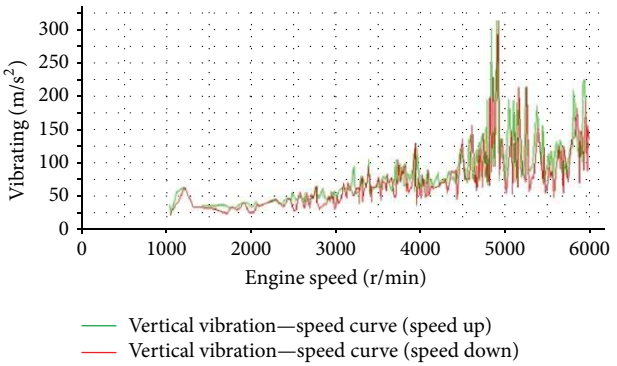

Figure 8: Experimental results.

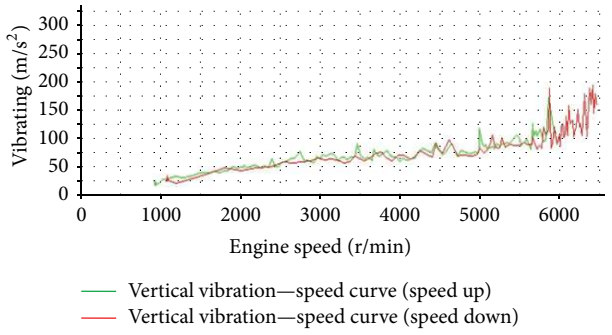

Figure 9: Experimental results.

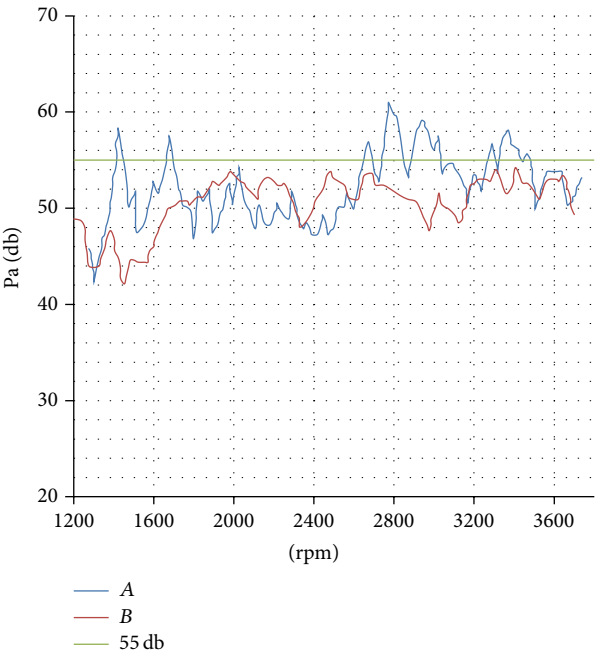

Figure 10: Experimental results: noise test inside vehicle. (*A*: noise effect; the angle of transmission shafts is 7° and the intermediate support stiffness is approximately 700 N/mm; *B*: noise effect; the angle of transmission shafts is 5° and the intermediate support stiffness is approximately 500 N/mm).

in this research, the installation angle between transmission shafts should be designed to be 5° as far as possible and the intermediate support stiffness should be 500 N/mm as predicted by theory and verified experimentally. As a result, the transmission shaft's effect on vibration and noise from the main reducer can be decreased. There is no other problem caused after long-term test. The method applied in this research has reference value for vibration and noise reduction in variable axial transmission systems.

Conflict of Interests

The authors declare that there is no conflict of interests regarding the publication of this paper.

Acknowledgment

It was partially supported by the WUT Innovation Fund 145204003.

References

[1] B. Gao, H. Chen, Y. Ma, and K. Sanada, "Design of nonlinear shaft torque observer for trucks with automated manual transmission," *Mechatronics*, vol. 21, no. 6, pp. 1034–1042, 2011.

[2] T. P. Turkstra and S. E. Semercigil, "Vibration control for a flexible transmission shaft with an axially sliding support," *Journal of Sound and Vibration*, vol. 206, no. 4, pp. 605–610, 1997.

[3] C. L. Yu, L. Zhang, J. G. Wu, and Z. J. Xie, "Modeling and simulation of a mini-bus with dynamics of multi-body systems," *Journal of Chongqing University*, vol. 26, pp. 35–38, 2003.

[4] M. Gnanakumarr, S. Theodossiades, H. Rahnejat, and M. Menday, "Impact-induced vibration in vehicular driveline systems: theoretical and experimental investigations," *Proceedings of the Institution of Mechanical Engineers Part K: Journal of Multi-Body Dynamics*, vol. 219, pp. 1–12, 2005.

[5] J. L. Xu, "Analysis of contact stress of hypoid gear of micro-car real rear axle," in *Proceedings of the 2nd International Conference on Electronic & Mechanical Engineering and Information Technology (EMEIT '12)*, vol. 9, pp. 949–954, 2012.

[6] K. Liu, *Research of the Soft Body Dynamics of the Gears in Main Reducer of Car Drive Axle*, Wuhan University of Technology, Wuhan, China, 2012.

[7] J. Baumann, D. D. Torkzadeh, A. Ramstein, U. Kiencke, and T. Schlegl, "Model-based predictive anti-jerk control," *Control Engineering Practice*, vol. 14, no. 3, pp. 259–266, 2006.

[8] L. Webersinke, L. Augenstein, and U. Kiencke, "Adaptive linear quadratic control for high dynamical and comfortable behavior of a heavy truck," SAE Technical Paper 0534, 2008.

[9] A. Artoni, M. Gabiccini, and M. Kolivand, "Ease-off based compensation of tooth surface deviations for spiral bevel and hypoid gears: only the pinion needs corrections," *Mechanism and Machine Theory*, vol. 61, pp. 84–101, 2013.

[10] D. Park, M. Kolivand, and A. Kahraman, "Prediction of surface wear of hypoid gears using a semi-analytical contact model," *Mechanism and Machine Theory*, vol. 52, pp. 180–194, 2012.

[11] Q. Wang and Y.-D. Zhang, "Coupled analysis based dynamic response of two-stage helical gear transmission system," *Journal of Vibration and Shock*, vol. 31, no. 10, pp. 87–91, 2012.

[12] W. W. Zheng, *Mechanical Principle*, Higher Education Press, Beijing, China, 1997.

[13] Z. Y. Zhu, *Theoretical Mechanics (I)*, Peking University Press, Beijing, China, 1984.

[14] Q. Li and J. J. Zhang, "Analysis and arrangement of mine car driveline system," *Mechanical Research & Application*, vol. 4, pp. 56–61, 2010.

[15] L. H. Wang, Y. Y. Huang, and Y. F. Li, "Study on nonlinear vibration characteristics of spiral bevel transmission system," *China Mechanical Engineering*, vol. 18, no. 3, pp. 260–264, 2007.

[16] L. Liu, *Finite Element Analysis of Car Propeller Shaft Supporting Bracket*, vol. 1, Drive Systems Technology, Shanghai, China, 2007.

[17] O. D. Mohammed, M. Rantatalo, and J.-O. Aidanpää, "Improving mesh stiffness calculation of cracked gears for the purpose of vibration-based fault analysis," *Engineering Failure Analysis*, vol. 34, pp. 235–251, 2013.

[18] M. Pang, X.-J. Zhou, and C.-L. Yang, "Simulation of nonlinear vibration of automobile main reducer," *Journal of Zhejiang University (Engineering Science)*, vol. 43, no. 3, pp. 559–564, 2009.